Bulletin of Earthquake Engineering
https://doi.org/10.1007/s10518-019-00635-y

ORIGINAL RESEARCH

Vertical ground motion prediction equations and vertical-to-horizontal (V/H) ratios of PGA and PSA for Algeria and surrounding region

Nasser Laouami[1]

Received: 31 December 2018 / Accepted: 30 April 2019

Abstract
The paper presents a ground motion prediction equation (GMPE) for the vertical pseudo spectral acceleration for periods varying from 0.02 to 4 s. The model is derived from the same strong motion database as previously considered for the horizontal GMPE for Algeria (Laouami et al. 2018). 583 vertical records homogeneously processed having magnitude and distance intervals of 3–7.4 and 1–150 km respectively are used. The functional forms are similar to those used for our horizontal GMPEs. To consider the soil factor, three soil classes are defined based on the horizontal over vertical spectral ratios: rock, firm and soft. Estimates of period-dependent site coefficients reveal negligible vertical site amplifications compared to the horizontal ones. This work also presents a model for vertical over horizontal (V/H) response spectral ratio derived from the vertical and the horizontal GMPEs. One found, particularly for small distances and large magnitudes, that the V/H ratio has a large peak, which may exceed unity, around the period range 0.04–0.1 s. This result may be very important for seismic behavior of stiff structures which vertical fundamental period's lies within a period range 0.04–0.15 s. The derived horizontal and vertical GMPE's are used to compute predicted H/V spectral ratios for given scenarios. Compared to the recorded mean H/V spectral ratios, this tool allows checking the confidence level of the site classification scheme. Comparison of the median V/H response spectral ratios with period predicted from the model of this study with those from the Algerian seismic code RPA99 (2003) and the EC-8 (2004) (type 1 and type 2) reveals that the definition of the V/H spectral ratio from the RPA99 is closer to the scenario ($M = 7$ and $R_{jb} = 100$ km). Unfortunately, this scenario is not the worst for the vertical component. The present study has shown that the worst case scenario is related to high magnitude and short distance. For this scenario, for which the RPA99s do not provide an adequate V/H ratio, the EC-8 type 1 appears to give higher values. The proposed vertical GMPE for Algeria is compared with recent published models. It results that the present model with those from Cagnan et al. (2016) and Stewart et al. (2016) are the most recommended for the seismic hazard analysis in Algeria.

Keywords Algerian strong ground motion · Vertical GMPE · Site effect · V/H spectral ratio · H/V spectral ratio · Design codes

✉ Nasser Laouami
nlaouami@cgs-dz.org

Extended author information available on the last page of the article

Published online: 07 May 2019

1 Introduction

Post-earthquake observations show that the vertical component ground motions can cause serious damage to structures such as bridges, dams and nuclear installations (Kunnath et al. 2008). For example, destructive earthquakes such as the Northridge, California (1994), Kobe, Japan (1995), and Chi–Chi, Taiwan (1999) showed very clear evidence that the vertical component recorded during these earthquakes was responsible for the extensive damage (Haji-Soltani et al. 2017). Also, the recordings have shown that the vertical component can equal or exceed the horizontal ground motion component. Therefore, from an engineering point of view, it becomes necessary to take into account, in a more realistic way, the vertical component when designing the structures. Actually, most of the codes worldwide assume the seismic vertical component to be 2/3 of the horizontal component as originally proposed by Newmark and Hall (1982), and sometimes ½ as in the Algerian code RPA99 (2003). As a result, all components of motion have the same frequency content in almost all design codes. Also, the 2/3 rule for V/H is unconservative in the near-field and over-conservative at large epicentral distances (Bommer et al. 2011, Akkar et al. 2014, Stewart et al. 2016).

The vertical design spectra in a probabilistic seismic hazard assessment can be developed in two ways (Gülerce and Abrahamson 2011): (i) use a vertical-to-horizontal spectral acceleration (V/H) ratio model to scale the horizontal spectrum that was developed using the results of the horizontal component PSHA, or (ii) compute the hazard for vertical ground motions using vertical ground-motion prediction equations (GMPEs) following the same approach used for the horizontal component. The first approach consists to empirically develop a GMPE directly for the V/H spectral ratio using V/H ratios from recorded data (e.g., Bozorgnia and Campbell 2004; Bommer et al. 2011; Edwards et al. 2011; Akkar et al. 2014; Bozorgnia and Campbell 2016). V/H GMPE's are typically used to modify a horizontal response spectrum (uniform hazard spectrum or scenario spectrum) to produce a corresponding vertical spectrum. The second approach is to empirically develop vertical GMPE using the same database and functional form as for the horizontal GMPE (Berge Thierry et al. 2003; Ambraseys et al. 2005; Bozorgnia and Campbell 2016; Stewart et al. 2016).

In this paper, considering the arguments detailed in Stewart et al. (2016), we used the second approach of developing a vertical GMPE. The model gives the 5% damped pseudo acceleration response spectra at periods ranging from 0.02 to 4 s. As for the horizontal GMPEs, recently developed by Laouami et al. (2018), similar database and functional form are used and therefore the equations derived for vertical motions are consistent with those derived for horizontal motions and allows a reliable computation of both the H/V and the V/H spectral ratios.

In the Algerian design code (RPA99 2003), the vertical response spectrum is specified simply as ½ of the horizontal spectrum. Based on the work of Elnashai and Papazoglu (1997), the EC8 (Eurocode 8 2004) has defined a vertical spectrum that is different from the horizontal one.

The data contain 583 vertical records homogeneously processed with 257 from Algeria, 247 from Europe and 79 from USA. The magnitude and distance range from 3.0 to 7.4 and 5 to 150 km respectively. Only shallow crustal earthquakes are considered, well distributed in terms of moment magnitude and hypocentral distance. Zhao et al. (2006) soil classification approach is used for the classification of the recording sites into 3 classes which are: rock, firm and soft. This work also presents a model for vertical to horizontal (V/H)

Table 1 Classification site based on site natural period (Zhao et al. 2006)

Site class	Site natural period (s)	Average shear wave velocity (m/s)	Corresponding EC-8 class	Corresponding RPA2003 class
SCI	$T_g < 0.20$ s	$Vs_{30} > 600$	A	S1
SCII	$0.20\ s \le T_g < 0.40$ s	$300 < Vs_{30} \le 600$	B	S2
SCIII	$0.40\ s \le T_g < 0.60$ s	$200 < Vs_{30} \le 300$	C	S3
SCIV	$T_g \ge 0.60$ s	$Vs_{30} \le 200$	D	S4

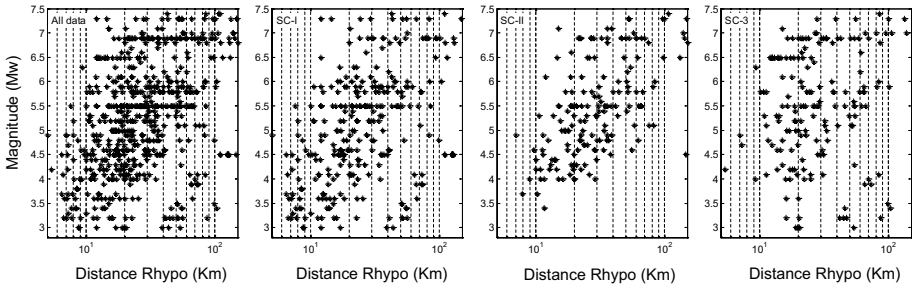

Fig. 1 Magnitude-distance distribution of data

response spectral ratio derived as the ratio of median predictions from the present vertical model and the already developed horizontal-component GMPEs. The obtained results are compared with the Algerian code RPA99 (2003) and the European design code EC-8 (Eurocode 8 2004).

2 Strong motion database

In this paper one uses the same strong motion database as in Laouami et al. (2018). The data contain 583 vertical records homogeneously treated with 257 from Algeria, 247 from Europe and 79 from USA. The hypocentral distance and moment magnitude ranges are 5–150 km and 3.0–7.4 respectively (earthquakes list, and the processing approach of the recorded data are found in Laouami et al. 2018). The pseudo spectral acceleration are computed for period T = 0.02 to 4 s appropriate for earthquake engineering applications.

The site effect analysis of the recorded data has already been addressed in Laouami et al. (2018). In Algeria, V_{S30} for strong-motion recording stations is not available. One used site class (SC) based on site period according to the classification scheme developed by Zhao et al. (2006) (Table 1). 4 site classes are defined rock (SCI), firm (SCII), soft (SCIII) and very soft (SCIV).

Figure 1 and Table 2 show the distributions of the magnitude-distance related to each site class of the 583 accelerograms and the corresponding record number respectively. Because the low number of data for SCIV one combines the SCIII and SCIV soil classes into a unique soil class named SC3 (SCIII + SCIV). According to the magnitude-distance distributions of Fig. 1 and the associated record number in Table 2, the data obtained seem to be representative of each of the considered soil classes.

Table 2 Number of vertical records corresponding to the 3 soil class

Site class	No. of records	EC-8	RPA99
SCI	324	A	S1
SCII	177	B	S2
SC3	173	C + D	S3 + S4

3 Functional form

The present study used functional forms similar to those used for our horizontal GMPEs (Laouami et al. 2018). The general functional form is given by:

$$\log_{10} \mathrm{PSA(T)} = \mathrm{a(T)} \cdot \mathrm{M_w} + \mathrm{b(T)} \cdot \mathrm{d} - \log_{10} \mathrm{d} + \mathrm{c_{1,2,3}(T)} + \sigma\mathrm{(T)} \quad (1)$$

in which PSA is the pseudo spectral acceleration, $a(T).M_w$ is the source parameter, $b(T).d-\log_{10}d$ is the path term, $c_{1,2,3}(T)$ is the site factor, and $\sigma(T)$ is the standard deviation. d is the hypocentral distance in Km, M_w the moment magnitude, a, b, c_1, c_2, and c_3 are period dependent regression coefficient, and T is the period in sec. The site terms c_1, c_2 and c_3 are for rock (SCI), firm (SCII) and soft (SC3) sites respectively.

The general form predicts the seismic motion response spectrum. The source term considers both the geometrical spreading and the anelastic attenuation. Two step regression analysis, which considers independently the magnitude and the distance, is performed for the whole data (Fukushima and Tanaka 1990, 1992; Joyner and Boore 1981).

Table 3 presents the obtained period-dependent regression coefficients. The standard deviation of the PGA is around 0.2809, very close to the one already obtained for the horizontal GMPEs, 0.2849. This result allows calculating the average ratios V/H with good confidence, since the horizontal and vertical standard deviations are very close. The distance parameter, b, exhibit positive values for $T > 0.75$ s. According to Spudich et al. (1997), and as we did for the horizontal GMPE, one reset the positive values of b to zero.

4 Results analysis

4.1 Comparison between the vertical and the horizontal GMPE's

As previously described, the empirical form of the vertical GMPE depends on three fundamental terms, the magnitude that represents the seismic source term, the distance for the path term, and the site class for the site effect term. The effects of each of those parameters on the vertical GMPE and also on the horizontal GMPE derived from the same database are shown in Fig. 2. Figure 2a shows the predicted vertical (solid line) and horizontal (dashed line) PSA with period for $M = 7$ at SC-1 rock site for $R_{jb} = 1$, 20 and 30 km. For this section and the following sections, the Joyner and Boore distance (R_{jb}), obtained by conversion of the hypocentral distance (R_{hyp}), is used (Sabetta et al. 2005; Laouami et al. 2018).

It is clear that the effect of the distance on the difference between the horizontal and the vertical spectral amplitudes lies in the period interval $T = 0.04$–0.09 s. The vertical spectral amplitude becomes close to the horizontal ones for distances less than 20 km while for small distances (< 5 km), the vertical spectral amplitude can exceed the horizontal ones.

Table 3 Period dependent regression coefficients for the vertical GMPE

T (s)	a	b	c_1	c_2	c_3	σ
PGA	0.4256	−0.0021	0.6493	0.6893	0.6487	0.2809
0.0200	0.4110	−0.0023	0.7614	0.7990	0.7426	0.2895
0.0300	0.3713	−0.0029	1.0880	1.1080	1.0520	0.3146
0.0400	0.3584	−0.0035	1.2840	1.2940	1.2330	0.3227
0.0500	0.3743	−0.0041	1.2880	1.3050	1.2440	0.3340
0.0600	0.3915	−0.0039	1.2150	1.2290	1.1780	0.3173
0.0700	0.3994	−0.0037	1.1750	1.1860	1.1510	0.3129
0.0800	0.4086	−0.0033	1.1200	1.1230	1.1080	0.3088
0.0900	0.4202	−0.0031	1.0430	1.0680	1.0570	0.3106
0.1000	0.4261	−0.0026	0.9793	1.0160	1.0090	0.3037
0.1100	0.4332	−0.0023	0.9156	0.9587	0.9469	0.3046
0.1200	0.4473	−0.0020	0.8189	0.8675	0.8508	0.3033
0.1300	0.4618	−0.0020	0.7178	0.7757	0.7588	0.3042
0.1400	0.4714	−0.0018	0.6381	0.6961	0.6864	0.3067
0.1500	0.4779	−0.0015	0.5769	0.6315	0.6162	0.3111
0.1600	0.4829	−0.0014	0.5243	0.5842	0.5706	0.3109
0.1700	0.4885	−0.0012	0.4757	0.5452	0.5181	0.3165
0.1800	0.4949	−0.0011	0.4212	0.4951	0.4657	0.3190
0.1900	0.5031	−0.0011	0.3543	0.4355	0.4048	0.3192
0.2000	0.5098	−0.0009	0.2918	0.3756	0.3463	0.3241
0.2500	0.5454	−0.0006	0.0141	0.0722	0.0326	0.3400
0.2800	0.5581	−0.0005	−0.1041	−0.0466	−0.0931	0.3476
0.2900	0.5646	−0.0006	−0.1581	−0.1033	−0.1455	0.3488
0.3000	0.5705	−0.0006	−0.2045	−0.1538	−0.1934	0.3482
0.3500	0.6047	−0.0005	−0.4626	−0.4479	−0.4453	0.3595
0.4000	0.6256	−0.0001	−0.6344	−0.6284	−0.5976	0.3719
0.4500	0.6533	−0.0002	−0.8520	−0.8512	−0.8096	0.3772
0.5000	0.6651	−0.0002	−0.9807	−0.9750	−0.9304	0.3794
0.5500	0.6871	0.0	−1.1550	−1.1470	−1.1000	0.3791
0.6000	0.7004	0.0	−1.2680	−1.2590	−1.2100	0.3799
0.6500	0.7202	0.0	−1.4350	−1.4160	−1.3450	0.3863
0.7000	0.7317	0.0	−1.5370	−1.5170	−1.4400	0.3903
0.7500	0.7470	0.0	−1.6580	−1.6450	−1.5730	0.3903
0.8000	0.7556	0.0	−1.7490	−1.7310	−1.6590	0.3918
0.8500	0.7661	0.0	−1.8420	−1.8150	−1.7470	0.3950
0.9000	0.7786	0.0	−1.9440	−1.9090	−1.8450	0.3973
1.0000	0.7971	0.0	−2.1110	−2.0620	−2.0130	0.3990
1.1000	0.8159	0.0	−2.2770	−2.2330	−2.1800	0.4033
1.2000	0.8322	0.0	−−2.4280	−2.3800	−2.3220	0.4070
1.2500	0.8396	0.0	−2.4960	−2.4430	−2.3840	0.4081
1.3000	0.8461	0.0	−2.5590	−2.5060	−2.4410	0.4094
1.4000	0.8583	0.0	−2.6670	−2.6260	−2.5490	0.4115
1.4500	0.8617	0.0	−2.6960	−2.6570	−2.5760	0.4115
1.5000	0.8690	0.0	−2.7630	−2.7300	−2.6410	0.4159

Table 3 (continued)

T (s)	a	b	c_1	c_2	c_3	σ
1.6000	0.8789	0.0	− 2.8600	− 2.8340	− 2.7370	0.4199
1.6500	0.8821	0.0	− 2.9090	− 2.8810	− 2.7850	0.4198
1.8000	0.8906	0.0	− 3.0090	− 2.9810	− 2.8970	0.4231
2.0000	0.8962	0.0	− 3.1270	− 3.0830	− 3.0040	0.4302
2.2000	0.9048	0.0	− 3.2420	− 3.1890	− 3.1170	0.4340
2.4000	0.9165	0.0	− 3.3560	− 3.2990	− 3.2500	0.4384
2.5000	0.9207	0.0	− 3.4060	− 3.3510	− 3.2980	0.4396
2.6000	0.9243	0.0	− 3.4540	− 3.4000	− 3.3440	0.4401
2.8000	0.9283	0.0	− 3.5380	− 3.4820	− 3.4240	0.4420
3.0000	0.9328	0.0	− 3.6170	− 3.5630	− 3.4990	0.4437
3.2000	0.9395	0.0	− 3.7070	− 3.6600	− 3.5860	0.4453
3.3000	0.9439	0.0	− 3.7650	− 3.7190	− 3.6420	0.4472
3.4000	0.9451	0.0	− 3.7900	− 3.7440	− 3.6650	0.4487
3.6000	0.9455	0.0	− 3.8490	− 3.7980	− 3.7140	0.4509
3.8000	0.9447	0.0	− 3.9090	− 3.8500	-3.7640	0.4516
4.0000	0.9421	0.0	− 3.9520	− 3.8920	− 3.8080	0.4487

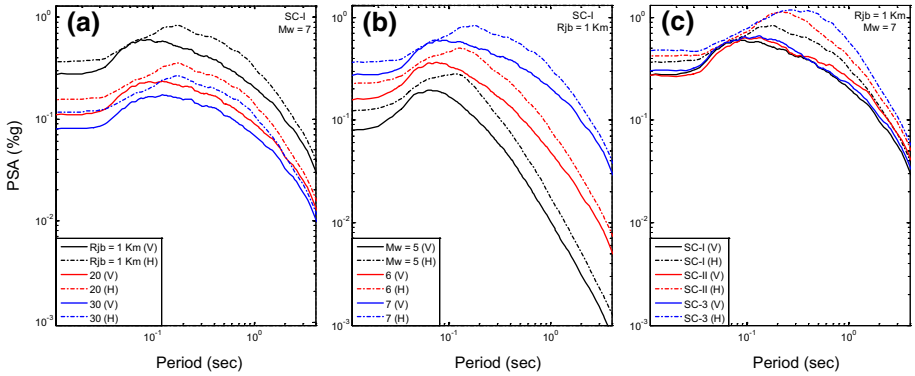

Fig. 2 Comparison between horizontal and vertical GMPE's with period

Figure 2b plots the magnitude variation effect on the horizontal and the vertical PSA at rock site (SCI) for $R_{jb} = 1$ km. As for the distance effect, one observe that the effect of the magnitude on the difference between the horizontal and the vertical spectral amplitudes lies in the same period interval T = 0.04–0.09 s. For the considered scenario ($R_{jb} = 1$ km), the vertical spectral amplitude becomes close to the horizontal ones for magnitude from 6 while for large magnitude (M = 7), the vertical spectral amplitude can exceed the horizontal ones. Figure 2c plots the soil class effect on the horizontal and vertical PSA for M = 7 reverse faulting earthquake and for $R_{jb} = 1$ km. Unlike the distance and magnitude effects analyzed above, it appears that the soil class has no effect on both the horizontal and the vertical spectral amplitudes in the period interval T = 0.04–0.09 s. This observation remains valid for the entire period interval for the vertical component, unlike the horizontal component which is clearly affected by the site effect for T > 0.1 s.

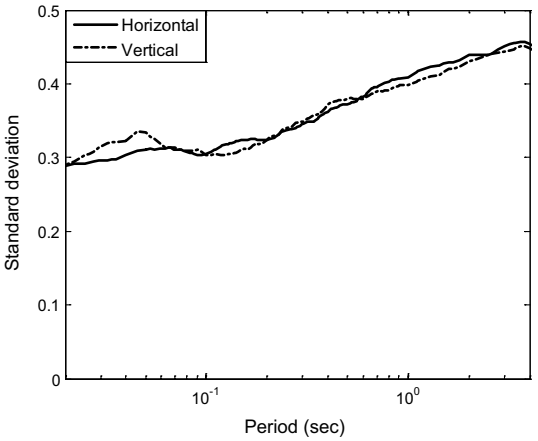

Fig. 3 Comparison of the standard deviations versus period for the horizontal and vertical GMPEs

In Fig. 3, the variation versus period of the standard deviations for both the vertical and the horizontal GMPE's are very close particularly for the PGA, $\sigma_H = 0.2809$ and $\sigma_V = 0.2849$. For periods between 0.02 and 0.06 s the vertical standard deviation is slightly larger than the horizontal one. This result may of interest when developing the ratio V/H, because for application to a UHS or to a scenario spectrum, only the median values of the V/H ratios are required, which makes the implicit assumption that the aleatory variability associated with the prediction of the vertical component is equal to that associated with the horizontal component (Bommer et al. 2011).

4.2 Dependent period site coefficients

Dependent period site coefficients, defined as the relative amplification with respect to SCI rock soil class, are computed for SCII and SC3 soil classes as follows:

$$\mathrm{ScII(T)} = \frac{\mathrm{PSA}^{\mathrm{SC\text{-}II}}(\mathrm{T})}{\mathrm{PSA}^{\mathrm{SC\text{-}I}}(\mathrm{T})}$$

$$\mathrm{Sc3(T)} = \frac{\mathrm{PSA}^{\mathrm{SC\text{-}3}}(\mathrm{T})}{\mathrm{PSA}^{\mathrm{SC\text{-}I}}(\mathrm{T})}$$

Figure 4 shows the site coefficients for SCII and SC3 soil classes obtained from the horizontal and vertical models. The plotted curves show that the predicted horizontal site coefficients (dashed line) have large peaks at periods T = 0.26 s and 0.5 s for SCII and SC3 soil classes respectively. However, the predicted vertical site coefficients (solid line) have slight peaks for period T = 0.1–0.2 s (i.e. 5–10 Hz) and 0.15–0.3 s (i.e. 3–6 Hz) for SCII and SC3 soil classes respectively. The most striking feature is that the peak periods for the vertical model are much smaller than those for the horizontal model. This is probably because vertical ground motions are generally of short periods than horizontal ground motions. Table 4 shows the vertical and the horizontal site amplification peak amplitudes and the related periods. Compared to the horizontal site amplification, the vertical one appears to be negligible and occur at low periods. The spectral period of the trough is about 0.05 s for the vertical model and is about 0.07 s for the horizontal model for both the 2 soil classes

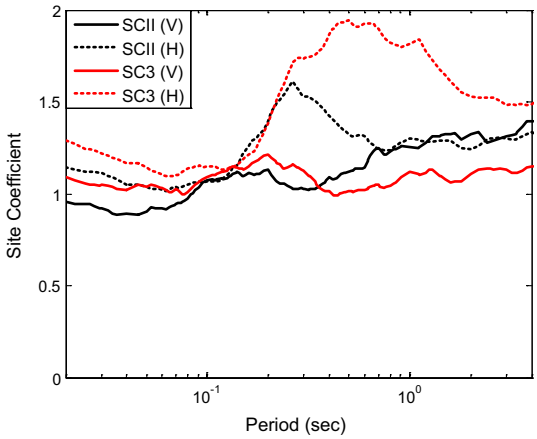

Fig. 4 Site coefficients versus period for SCII and SC3 soil classes. H and V denote horizontal and vertical components

Table 4 Site coefficient Peak amplitudes and related periods for the horizontal and vertical models

	Period (s)		Peak amplitude	
	SCII	SC3	SCII	SC3
Horizontal	0.26	0.5	1.61	1.94
Vertical	0.15	0.2	1.12	1.20

SC-2 and SC3. The trough period may be interpreted as the average site periods for the SCI sites (rock soil) as observed by Zhao et al. (2017).

4.3 Predicted horizontal over vertical spectral ratio

As described in Sect. 2, the site effect was introduced by applying to the considered recording stations a site classification scheme described in Table 1. In this section, in order to check the confidence level of the site classification approach used to develop the horizontal (Laouami et al. 2018) and the actual vertical GMPEs, comparison is performed between the predicted H/V spectral ratio defined as the ratio between the horizontal and the actual vertical GMPEs and the recorded mean H/V spectral ratios defined for the 4 soil classes in Laouami et al. (2018). The main assumption of H/V method is that horizontal-component ground motions are amplified around the fundamental frequency of a site, whereas the vertical-component does not experience significant amplification. SESAME (2004) guidelines, which states that when the maximum peak amplitude H/V is less than or equal to 2, it means that the site is rocky, are used. In other words, for example for soil class SCI (Rock), the predicted H/V spectral ratio must give a rather flat curve synonymous of a non-amplifiable site whose fundamental peak amplitude must not exceed 2. If the amplification of the predominant period is found greater than 2, it means that the classification of the strong motions database was not entirely reliable and that the data recorded on other soil classes (SCII, SCIII or SCIV) were incorrectly classified in soil class SCI. Figure 5 compares the predicted horizontal over vertical spectral ratios with period for M = 6 reverse faulting moderate earthquake, and for near (R_{jb} = 10 km), intermediate (R_{jb} = 30 km) and far distances (R_{jb} = 50 km) at rock (top panels), firm (middle panels) and soft (bottom

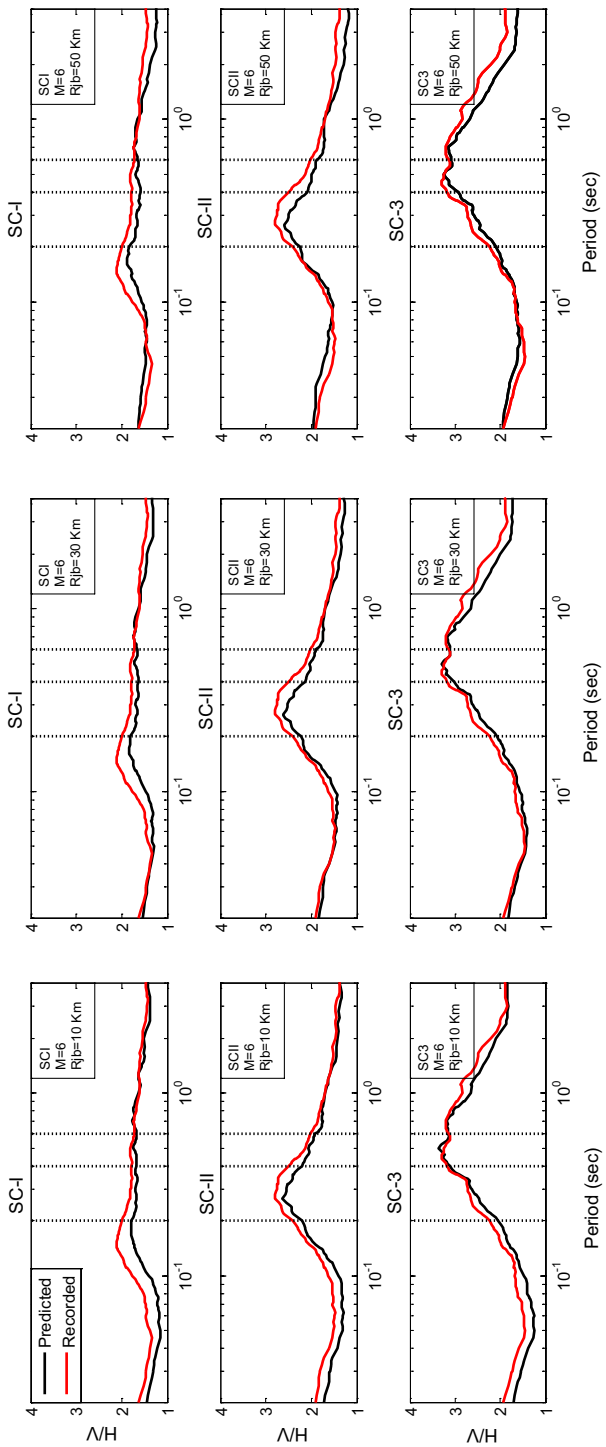

Fig. 5 Comparison between recorded and predicted H/V spectral ratios for M = 6 reverse faulting moderate earthquake, and for near (R_{jb} = 10 km), intermediate (R_{jb} = 30 km) and far distances (R_{jb} = 50 km), at rock (top panels), firm (middle panels) and soft (bottom panels) soil class. The period intervals (Table 1) are plotted with vertical dashed lines

panels) soil with the corresponding recorded mean H/V spectral ratios. In the same figure, one plot with vertical dashed lines the site natural periods defined in Table 1. Overall, the predicted and recorded curves are very close, for different soil classes and distances. It appears a high similarity between the predicted and the recorded mean H/V spectral ratios. Both give close amplifications, at the same site natural period ranges. For SCI, SCII and SC3 soil classes, the amplification occur at period ranges $T < 0.20$ s, $0.20\ s \leq T < 0.40$ s, and $0.40\ s \leq T$ s respectively. Likewise, the spectral amplitudes of the H/V spectral ratios are less than 2 for SCI, between 2 and 3 for SCII and greater than 3 for SC-3. This result reflects the reliability of the classification of the recording stations among the 4 soil classes.

Therefore, since the predicted H/V spectral ratios and the recorded ones are close for different scenarios and have peaks in the same period range to those defined for each site class in Table 1, it can be assumed that the horizontal and the vertical developed GMPEs have a rather reliable prediction. Estimation of the H/V spectral ratio from horizontal and vertical GMPEs developed from the same database can be a reliable indicator or "test" of the confidence level of the strong motions database classification.

4.4 Predicted vertical over horizontal spectral ratio

Variations of the predicted V/H response spectral ratios as a function of distance, magnitude, and soil class are presented in this section. The V/H spectral ratio is calculated for any seismic scenario as the ratio of median predictions from the present vertical GMPE and the horizontal GMPE (Laouami et al. 2018), developed from the same recordings database. Figure 6 shows the median V/H estimates for PGA (Fig. 6a, c) and $T = 0.06$ s (Fig. 6b, d) as a function of distance for a range of moment magnitude ($M_w = 5, 6, 7$) (Fig. 6a, b) and for different soil classes SCI, SCII and SC3 (Fig. 6c, d). According to Fig. 6a, b, the median V/H response spectral ratios reach their maximum in the near field ($R_{jb} < 10$ km) and decrease with distance, probably because the short-period vertical component attenuates rapidly than the horizontal component. Also, it is observed a smaller effect of the magnitude on the V/H spectral ratio related to the PGA (Fig. 6a) than at $T = 0.06$ s (Fig. 6b). For M5, M6 and M7, the maximum amplitudes reached by the median V/H are respectively 0.64, 0.69 and 0.75 for PGA and 0.78, 0.89 and 1.003 for $T = 0.06$ s. For $Mw = 7$, in the near field ($R < 5$ km), the vertical component is slightly larger than the horizontal one.

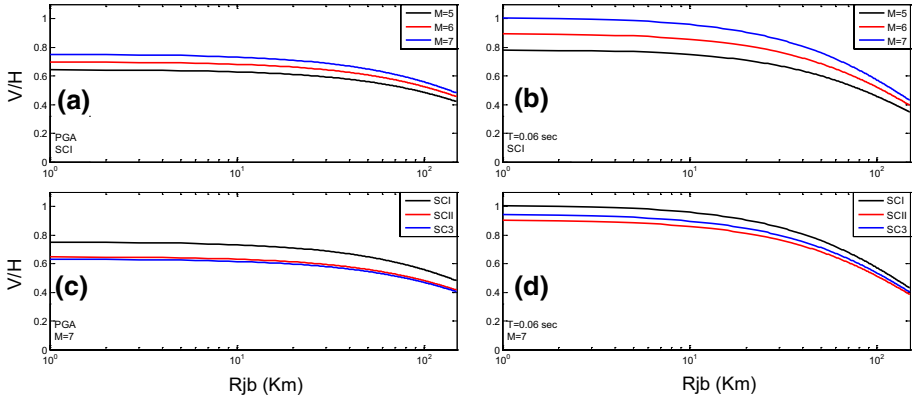

Fig. 6 Variation of the median V/H estimates versus distance for PGA (**a**, **c**) and $T = 0.06$ s (**b**, **d**)

Figure 6c, d show the soil class effect on the median V/H response spectral ratios for both PGA (Fig. 6c) and T = 0.06 s (Fig. 6d). Interestingly, the V/H ratio is larger for the rock site (SCI) than for the firm site (SCII) or the soft site (SC3). This is because the horizontal ground motion component record relatively small amplitudes on rocky sites (SCI) compared to the other sites (SCII and SC3), and at the same time, the vertical component seems little sensitive to this soils variability. The same trend is found by Bommer et al. (2011) and Haji-Soltani et al. (2017). Akkar et al. (2014) found that the V/H ratio increases with V_{s30} for small amplitudes (M = 4–5) and decreases for M > 6. Stewart et al. (2016) found that V/H drops in soft soils at large distances where non-linear effects are small.

Figure 7 illustrates the median V/H response spectral ratios as a function of period for ranges of magnitude (Fig. 7a), for range of distance (Fig. 7b) and for different soil classes (Fig. 7c). Figure 7a displays the period-dependent V/H variation for different magnitudes for R_{jb} = 5 km and for rock soil class (SCI). The plotted curves indicate that an increase in magnitude gives larger V/H peaks amplitude in the short-period range 0.04–0.2 s and for longer period 1–4 s, with a slight shift of the corresponding periods towards the high periods. For T < 0.04 s and for 0.2 < T < 1 s, the magnitude effect is negligible. The V/H spectral ratio peaks at around T = 0.04–0.1 s and attenuates rapidly with increasing period up to T = 0.2 s.

Figure 7b plot the period-dependent V/H variation for different distances for M_w = 7 and for rock soil class (SCI). The plotted curves indicate that V/H decrease as distance increases in the period range 0.03 < T < 0.15 s, becomes relatively flat with period, around 0.6 s, and relatively independent of the distance for 0.15 < T < 1.1 s, and increase with both distance and period for 1.1 < T < 4 s. For R_{jb} = 100 km, V/H spectral ratio markedly increases with period T. The same observations have been observed previously by Haji-Soltani et al. (2017) and Stewart et al. (2016), the authors observed that the increase of V/H with distance is a result of the vertical-component ground motions having slower rates of geometric spreading.

Figure 7c displays the period-dependent V/H variation for different soil classes for M_w = 7 and for R_{jb} = 5 km. For T < 0.1 s and 0.15 < T < 0.7 s, as indicated in Fig. 6c, d above, the V/H ratios is larger at rock site (SCI) than at firm (SCII) or soft sites (SC3). The site term does not influence the median V/H ratios for 0.1 < T < 0.15 s, while for T > 0.7 s, the median V/H spectral ratios for both SCI and SCII are close and larger than at SC3 soil class. The median V/H spectral ratio amplitudes for soil class SC3 are the lowest for T > 0.3 s, because in this period range, the horizontal component of the earthquake, characterized by long-period content, is generally amplified by the site effect phenomenon, unlike the vertical component characterized by short-periods content.

It follows from the foregoing, particularly for small seismic source-site distances and large magnitude, that the V/H spectral ratio peak can exceed unity, around the period range 0.04–0.1 s. This result may be important for the seismic behavior of stiff structures whose vertical fundamental period is in the range of 0.04–0.15 s (see Table 5 from Papazoglou and Elnashai 1996). It is important to note that Papazoglou and Elnashai (1996) found that some failure modes are due to the strong vertical seismic component.

4.5 Residuals

Residuals are computed for each observed value to determine how the data is adjusted by the prediction equation, with the expression: Y = log(GMobserved)–log(GMpredicted), with GMpredicted is the predicted ground motion computed with the GMPE for the

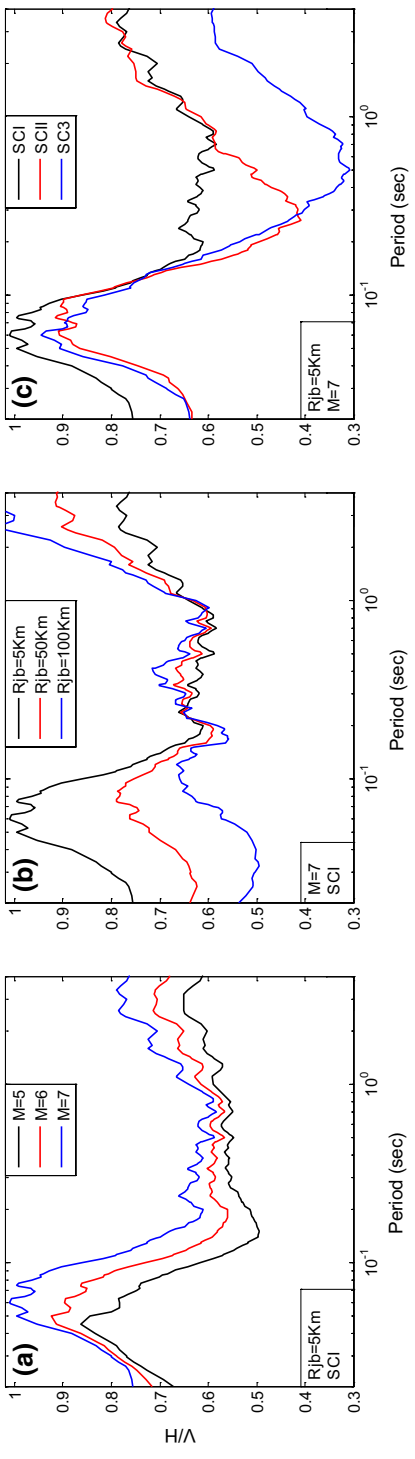

Fig. 7 Variation of the median V/H estimates versus period for different magnitude (**a**), distance (**b**) and soil classes (**c**)

Table 5 Fundamental horizontal and vertical natural periods of RC building (Papazoglou and Elnashai 1996)

Number floors	Horizontal period (s)	Vertical period (s)
1	0.1	0.040
2	0.2	0.064
3	0.3	0.082
4	0.4	0.091
5	0.5	0.099
6	0.6	0.106
7	0.7	0.114
8	0.8	0.120

magnitude M_w, distance R_{jb} and soil class SC of the observed ground motion GMobserved. The obtained residuals are plotted in Fig. 8 together with linear best-fit relations. The top and the bottom panels plot the variations of the residuals with M_w and R_{jb} respectively, for PGA, 2, 1 and 0.2 s periods. With respect to the magnitude, no significant trends are observed. For the distance, linear trends are found particularly at large distance (> 100 km) for 2 s natural period. This is due to the reduced amount of data in this distance range. All the residuals plots show no obvious dependence of the scatter on magnitude or distance. Despite the presence of some relative scarcity of data at longue period (T = 1–2 s), this apparent constant bias is common to all graphs of residuals for long period motions as related by Ambraseys et al. (2005). For the PGA, the residual values do not exhibit any systematic bias associated to a specific magnitude or distance.

4.6 Comparison to previous equations and codes

4.6.1 Predicted vertical spectral acceleration

The comparison is done with the predicted vertical ground motion from Ambraseys et al. (2005), Cagnan et al. (2016), and Stewart et al. (2016) developed in the same sismotectonic context i.e. shallow crustal earthquakes. Three magnitude levels (M5, M6 and M7) are used in the comparisons that can encompass small, moderate and strong earthquakes in Algeria and surrounding regions.

Figure 9 provides the comparison with the 03 models in term of PGA versus distance for M5, M6 and M7 at SCI rock site. For magnitudes M5, M6 and M7 and up to distances R10, R15 and R20 respectively, our model predictions are relatively smaller than that predicted by the other models. Our predictions are closer to Cagnan et al. (2016) and Stewart et al. (2016) models for M = 5, closer to Cagnan et al. (2016) for M = 6 and closer to Stewart et al. (2016) for M = 7. For large distances; relatively high PGA are predicted by the proposed model. The Ambraseys et al. (2005) model seems to predict large PGA at short distances.

In Fig. 10, comparison is made between the predicted PSA with Ambraseys et al. (2005), Cagnan et al. (2016) and Stewart et al. (2016) models. Scenarios are performed at SCI rock site for distances R5, R20, R30 km and M = 5.0, for R5, R30, R50 km and M = 6.0, and for R5, R50, R100 km and M = 7.0. For small distances (R5) and for magnitudes M5, M6 and M7, lower spectral accelerations are predicted by our model. For intermediate and far distances, and for magnitudes M5 and M6, a good similarity is observed

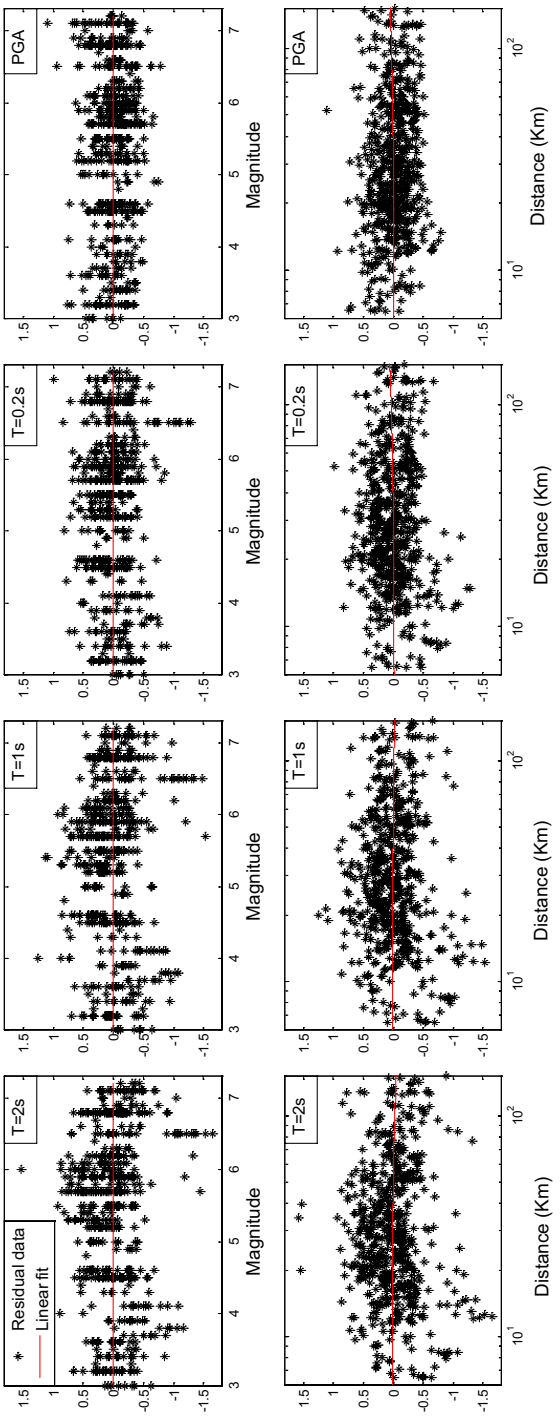

Fig. 8 Residuals against Magnitude (top panels) and distance (bottom panels)

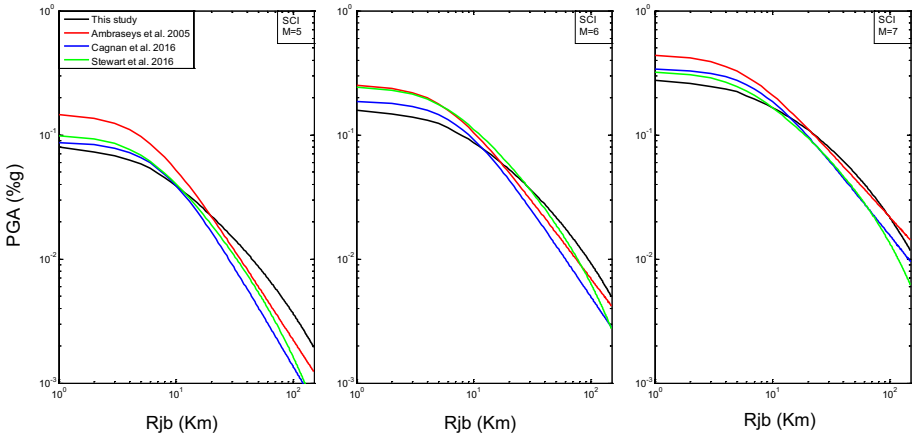

Fig. 9 Comparison of the PGA with distance for M5, M6 and M7at a rock site predicted from the model of this study (black lines) with those from Ambraseys et al. (2005), Stewart et al. (2016) and Cagnan et al. (2016)

with the models of Stewart et al. (2016) and Cagnan et al. (2016), while for magnitudes M7, the proposed model is close to the model of Ambraseys et al. (2005).

Figure 11 compares the predicted site coefficients obtained from the present study with the ones from Ambraseys et al. (2005), Cagnan et al. (2016) and Stewart et al. (2016) models. It should be noted that the model from Ambraseys et al. (2005) uses the same definition of the site factor based on soil class, while for Cagnan et al. (2016) and Stewart et al. (2016) models, the site classification is defined by the time-averaged shear wave velocity in the upper 30 m of the soil profile. For the comparison purpose, one uses $V_{s30} = 560$ m/s for SCII and 260 m/s for SC3. At firm soil (SCII), Fig. 11a reveals for $T > 0.1$ s that the site coefficient derived from our model is close to the other models, while for $T < 0.1$ s slight de-amplification is observed. At soft soil (SC3), Fig. 11b shows that the site effect does not influence the vertical component, except around the period $T = 0.2$ s, which shows slight amplification. On the other hand, the other models exhibit strong amplifications especially for long periods. It seems difficult to explain the difference between the amplification predicted by the proposed model and that predicted by the other models for soil class SC3. This amplification level observed from the other models, which is quite normal for the horizontal component, appears exaggerated for the vertical component which, because of its frequency content, is supposed less affected by the site effects. Moreover, the H/V spectral ratio approach is based on this assumption. According to Bindi et al. (2009), the site effects are mainly controlled by resonance phenomena, i.e. when the dominant period of the strong motion is close to the soil fundamental period. For soil class SC3, which is characterized by a period interval $T > 0.4$ s, this eventuality is unlikely, as the vertical component of the earthquake exhibits weaker periods.

Figure 12 show the comparison of the predicted median vertical response spectra with those from Ambraseys et al. (2005), Cagnan et al. (2016) and Stewart et al. (2016), at SCII and SC3 soil classes. Scenarios are performed for distances R5, R30, R50 km and $M = 6.0$. As expected, this comparison is closely related to the results shown in Fig. 11. Our model predicts spectral accelerations close to the other models for the firm site (SCII), whereas they are lower for soft soils (SC3) mainly for long periods.

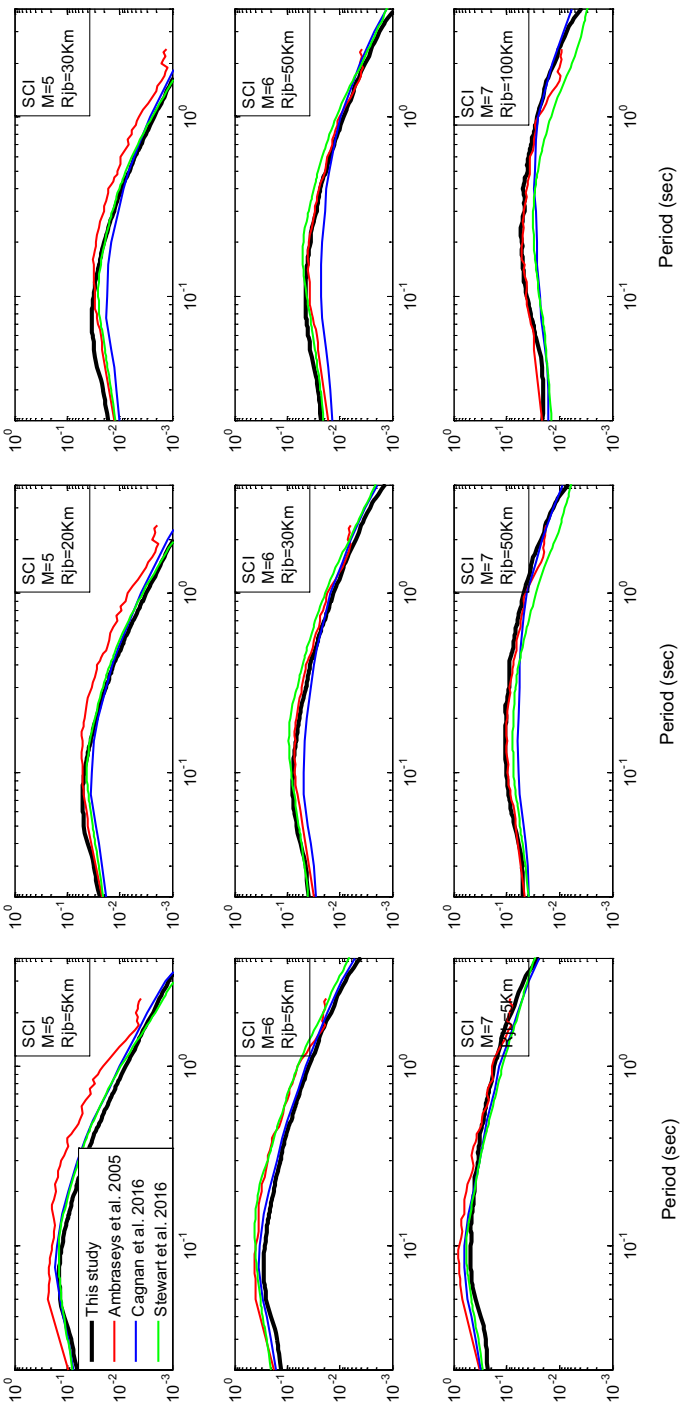

Fig. 10 Comparison of vertical pseudo spectral acceleration for M5, M6 and M7 SCI rock site predicted from the model of this study (black lines) with those from Stewart et al. (2016), Cagnan et al. (2016), and Ambraseys et al. (2005)

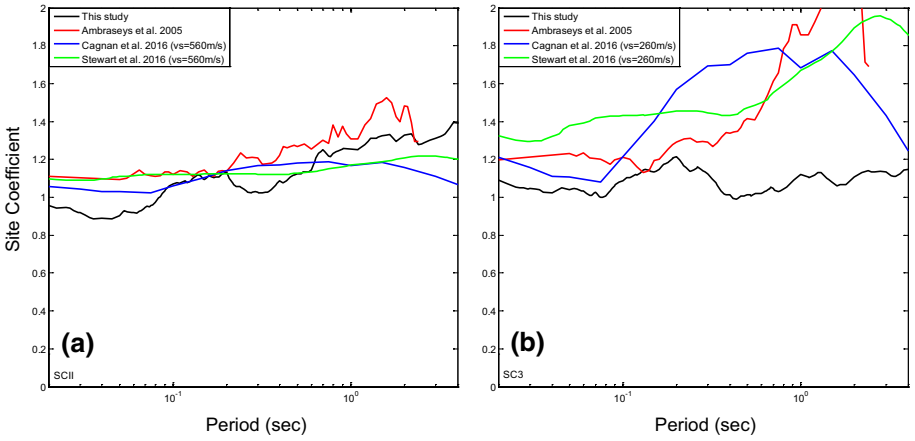

Fig. 11 Estimated site coefficients for **a** stiff soil sites (SCII) and **b** soft soil sites (SC3) from this study and some previous studies (Ambraseys et al. 2005; Cagnan et al. 2016; Stewart et al. 2016)

4.6.2 V/H spectral ratio

The V/H spectral ratio, constructed for any seismic scenario as the ratio of median predictions from the present vertical GMPE and the horizontal one (Laouami et al. 2018), developed from the same recordings database, is compared with the predicted V/H ratios from Bommer et al. (2011), Gülerce and Abrahamson (2011), Akkar et al. (2014), and Stewart et al. (2016). The first 3 models are direct predictions of the V/H ratio, while the fourth model is constructed from independents horizontal and vertical GMPEs derived from the same dataset. Figure 13 compares our predicted median V/H spectral ratios with those of Bommer et al. (2011), Gülerce and Abrahamson (2011), Akkar et al. (2014) and Stewart et al. (2016) for $R_{jb}=2$ km (top panels) and 30 km (bottom panels), at rock site (SCI), and for $M=5$, 6 and 7.0. In general, one observes that the 5 models follow fairly the same trend and show some variability more marked for $R_{jb}=2$ km. At this distance, for the short periods, our predicted V/H median falls between those of Stewart et al. (2016) and Gülerce and Abrahamson (2011). For $R_{jb}=30$ km, the difference between the 5 models is reduced and the proposed model predicts the highest V/H spectral ratios, mainly for $M=6$ and 7.

Figure 14 compares our predicted median V/H spectral ratios with those of Bommer et al. (2011), Gülerce and Abrahamson (2011), Akkar et al. (2014) and Stewart et al. (2016) for $R_{jb}=2$ km (top panels) and 30 km (bottom panels), at soft site (SC3), and for $M=5$, 6 and 7.0. For $R_{jb}=2$ km, as expected from Fig. 11, our model predicts the lowest V/H median spectral ratio together with the model of Bommer et al. (2011), while the models from Gülerce and Abrahamson (2011) and Stewart et al. (2016) predict the highest peak values. For $R_{jb}=30$ km, the predictions of the 5 models are close except for $M=7$, which shows higher V/H spectral ratios in short periods from the models of Stewart et al. and Gulerce and Stewart.

According to Bommer et al. (2011), there are few codes that have defined vertical spectra in agreement with the variation of the V/H ratio with response period. In this section, the predicted V/H spectral ratios are compared with 2 seismic codes, the Algerian code (RPA99 2003) which specified the vertical spectrum simply as the half of the horizontal one, and the EC-8 (2004) which considers a vertical spectrum independently from the

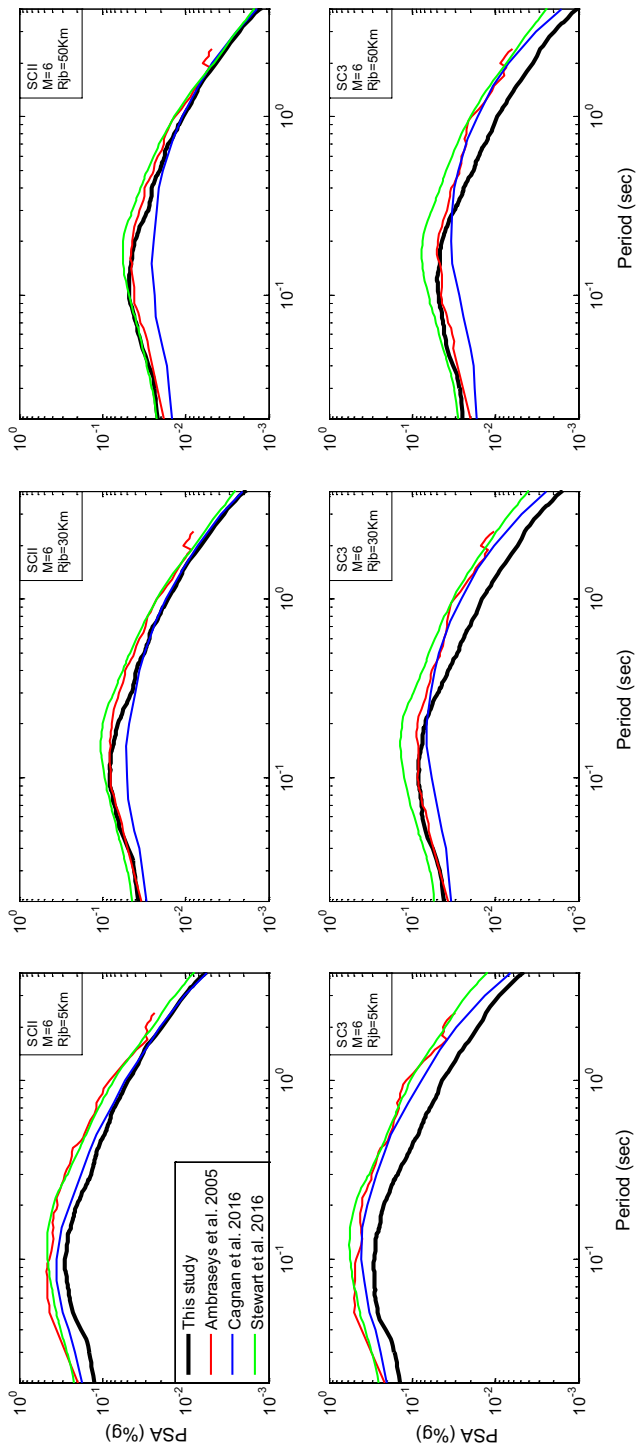

Fig. 12 Comparison of vertical pseudo spectral acceleration for magnitude M6 and different distances at a firm site (SCII, top panels) and soft site (SC3, bottom panels) predicted from the model of this study (black lines) with those from Stewart et al. (2016), Cagnan et al. (2016), and Ambraseys et al. (2005)

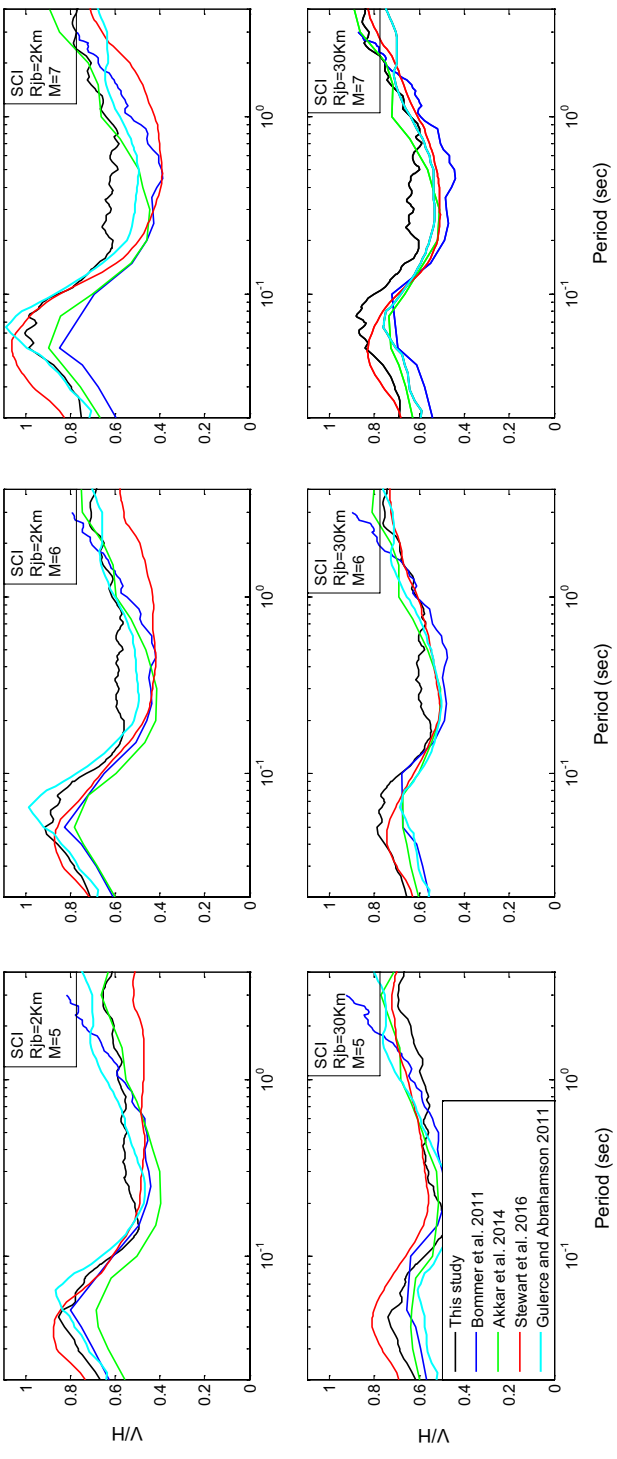

Fig. 13 Comparison of V/H response spectral ratios with period predicted from the model of this study at rock site (SCI) for $R_{jb} = 2$ km (top panels) and $R_{jb} = 30$ km (bottom panels) with those from Stewart et al. (2016), Akkar et al. (2014), Bommer et al. (2011) and Gülerce and Abrahamson (2011)

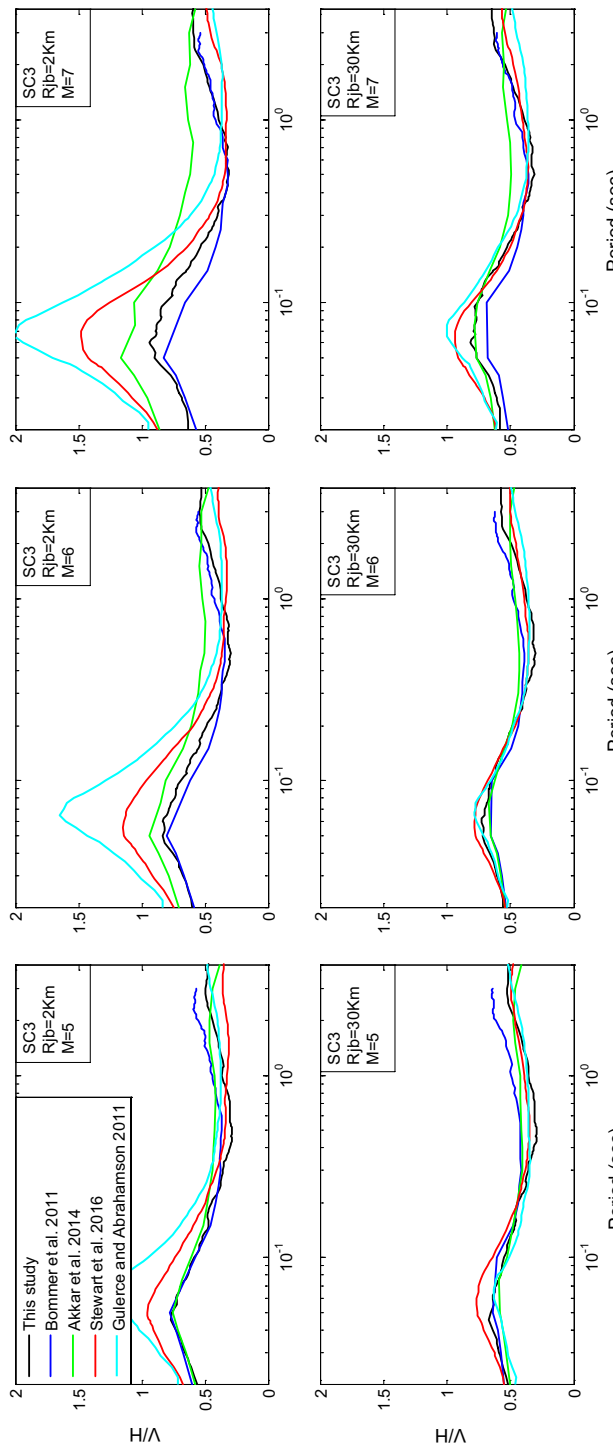

Fig. 14 Comparison of V/H response spectral ratios with period predicted from the model of this study at soft site (SC3) for $R_{jb} = 2$ km (top panels) and $R_{jb} = 30$ km (bottom panels) with those from Stewart et al. (2016), Akkar et al. (2014), Bommer et al. (2011) and Gülerce and Abrahamson (2011)

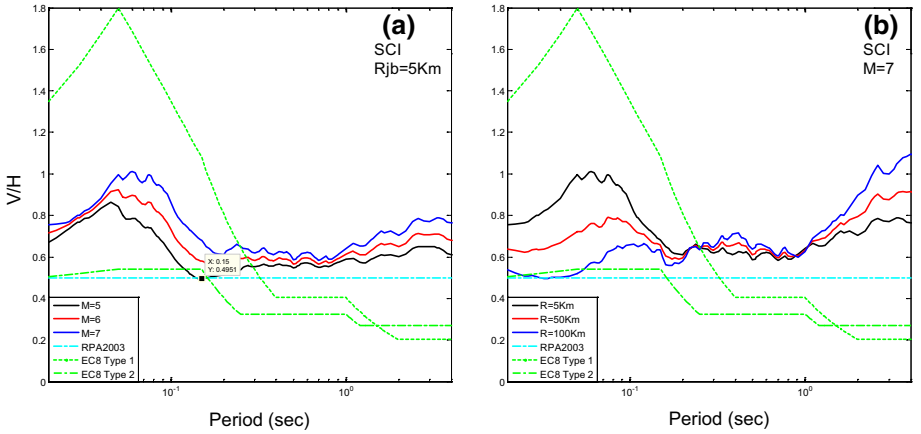

Fig. 15 Comparison of V/H response spectral ratios with period predicted from the model of this study at rock site (SCI) with those from the Algerian seismic code RPA99 (2003) and the EC8 (2004) for different magnitude (**a**) and different distance (**b**)

horizontal one. More details about V/H ratios from codes and regulations can be found in Bommer et al. (2011).

Figure 15 shows the comparison of the median V/H response spectral ratios with period predicted from the model of this study at rock soil class with those from the Algerian seismic code RPA99 (2003) and the EC-8 (2004) (type 1 and type 2) for different magnitude (M5, M6 and M7) (Fig. 15 a) and different distance (R5, R50 and R100) (Fig. 15 b).

In Fig. 15a, for $R_{jb}=5$ km, compared to the spectral ratios predicted by the proposed model, the V/H spectral ratios obtained from RPA99 and EC-8 (Type 2) give lower values, over the entire period range and for the considered magnitudes, except around $T=0.15$ s and $M=5$, while EC -8 (Type 1) gives very high values for $T<0.3$ s and lower values beyond 0.3 s.

In Fig. 15b, for $M=7$, the main result is that, for short periods, the spectral ratios obtained from RPA99 and EC-8 (type 2) are both close to the predicted H/V spectral ratio for the distance $R_{jb}=100$ km, whereas they give low values for shorter distances ($R_{jb}=5$ and 50 km).

The obtained results show that the definition of the V/H spectral ratio from the RPA99 is closer to the scenario ($M=7$ and $R_{jb}=100$ km). Unfortunately, this scenario is not the worst for the vertical component. The present study has shown that the worst case scenario is a high magnitude ($M=7$) and a short distance ($R_{jb}=5$ km). For this scenario, for which the RPA99 do not provide an adequate V/H ratio, the EC-8 type 1 appears to give higher values.

5 Conclusion

In this work, a vertical GMPE and V/H response spectral ratios for Algeria and surrounding region is presented. 583 vertical records homogeneously processed having magnitude and distance intervals of 3–7.4 and 1–150 km respectively are used. The presented model is the first model derived specifically for application in North Africa

region. To consider the soil factor, three soil classes are defined based on the horizontal over vertical spectral ratios approach and the adopted classification scheme (Table 1): rock, firm and soft. The results obtained highlight the following conclusions:

(i) The vertical model is derived from a database and a functional form previously used to develop the horizontal GMPE for Algeria (Laouami et al. 2018).
(ii) The derived period-dependent site coefficients for soil classes SCII and SC3 reveal negligible vertical site amplifications compared to the horizontal ones.
(iii) The standard deviation value of the PGA for the vertical GMPEs is very close to the one obtained for the horizontal GMPEs (Laouami et al. 2018). This result allows calculating the average V/H response spectral ratios with good confidence.
(iv) Estimating the H/V spectral ratios from horizontal and vertical GMPEs developed from the same database can be a reliable indicator or "test" of the confidence level of the recording stations classification and, therefore, the confidence level of the horizontal and vertical GMPE's. High similarity between the predicted and the recorded H/V spectral ratios is found for different scenarios (R_{jb}, M_w, Soil classes). Both give close amplifications, at the same site natural period ranges, according to the classification scheme. For SCI, SCII and SC3 soil classes, the amplification occur at period ranges $T < 0.20$ s, $0.20\ s \leq T < 0.40$ s, and $0.40\ s \leq T$ s respectively.
(v) For small distances and large magnitude, the V/H spectral ratio has a large peak, which may exceed unity, around the period range 0.04–0.1 s. This result may be very important for seismic behavior of stiff structures which vertical fundamental period's lies within a period range 0.04 s–0.15 s.
(vi) The comparison of our model estimations with those from the models of Ambraseys et al. (2005), Cagnan et al. (2016), and Stewart et al. (2016) shows that our predictions are slightly lower than the other models in near distances. Moreover, the present model with those from Cagnan et al. (2016) and Stewart et al. (2016) are the most recommended for the seismic hazard analysis in Algeria.
(vii) Comparison of our predicted median V/H response spectral ratios with those of Bommer et al. (2011), Gülerce and Abrahamson (2011), Akkar et al. (2014) and Stewart et al. (2016) reveals that the 5 models follow fairly the same trend. At rock site, our predicted V/H median falls between those of Stewart et al. (2016) and Gülerce and Abrahamson (2011), while at soft site, our model predicts the lowest V/H median spectral ratio together with the model of Bommer et al. (2011).
(viii) Comparison of the median V/H response spectral ratios with period predicted from the model of this study at rock soil class with those from the Algerian seismic code RPA99 (2003) and the EC-8 (2004) (type 1 and type 2) reveals that the definition of the V/H spectral ratio from the RPA99 is closer to the scenario ($M = 7$ and $R_{jb} = 100$ km). Unfortunately, this scenario is not the worst for the vertical component. The present study has shown that the worst case scenario is a high magnitude ($M > 6$) and a short distance ($R_{jb} < 10$ km). For this scenario, for which the RPA99 s do not provide an adequate V/H ratio, the EC-8 type 1 appears to give higher values.

Acknowledgements The author thanks the associate editor and the anonymous reviewers for their constructive criticism and comments that helped us to improve this study.

References

Akkar S, Sandıkkaya MA, Ay BO (2014) Compatible ground-motion prediction equations for damping scaling factors and vertical-to-horizontal spectral amplitude ratios for the broader Europe region. Bull Earthq Eng 12:517–547. https://doi.org/10.1007/s10518-013-9537-1

Ambraseys NN, Douglas J, Sarma SK, Smit PM (2005) Equations for the estimation of strong ground motions from shallow crustal earthquakes using data from Europe and the Middle East: vertical peak ground acceleration and spectral. Bull Earthq Eng 3:54–73

Berge Thierry C, Cotton F, Scotti O, Pommera DA, Fukushima Y (2003) New empirical response spectral attenuation laws for moderate European earthquakes. J Earthq Eng 7:193–222

Bindi D, Parolai S, Cara F, Di Giulio G, Ferretti G, Luzi L, Monachesi G, Pacor F, Rovelli A (2009) Site amplification observed in the Gubbio basin, central Italy: hints for lateral propagation effects. Bull Seismol Soc Am 99(2A):741–760

Bommer JJ, Akkar S, Kale O (2011) A model for vertical-to-horizontal response spectral ratios for Europe and the Middle East. Bull Seismol Soc Am 101(4):1783–1806. https://doi.org/10.1785/012010

Bozorgnia Y, Campbell KW (2004) The vertical-to-horizontal spectral ratio and tentative procedures for developing simplified V/H and vertical design spectra. J Earthq Eng 4:5–539

Bozorgnia Y, Campbell KW (2016) Ground motion model for the vertical-to-horizontal (V/H) ratios of PGA, PGV, and response spectra. Earthq Spectra 32:951–978

Cagnan Z, Akkar S, Kale O, Sandıkkaya A (2016) A model for predicting vertical component peak ground acceleration (PGA), peak ground velocity (PGV), and 5% damped pseudospectral acceleration (PSA) for Europe and the Middle East. Bull Earthq Eng. https://doi.org/10.1007/s10518-016-0063-9

Edwards B, Poggi V, Fah D (2011) A predictive equation for the vertical-to-horizontal ratio of ground motion at rock sites based on shear-wave velocity profiles from Japan and Switzerland. Bull Seismol Soc Am 101:2998–3019

Elnashai AS, Papazoglu AJ (1997) Procedure and spectra for analysis of RC structures subjected to vertical earthquake loads. J Earthq Eng 1(1):121–155

Eurocode 8 (2004) Design of structures for earthquake resistance—Part 1: general rules, seismic actions and rules for buildings. EN 1998-1: 2004. Comite Europeen de Normalisation, Brussels

Fukushima Y, Tanaka T (1990) A new attenuation relation for peak horizontal acceleration of strong earthquake in Japan. Bull Seism Soc Am 80:757–783

Fukushima Y, Tanaka T (1992) Revised attenuation relation of peak horizontal acceleration by using a new data base. Prog Abstr Seism Soc Jpn 2:116

Gülerce Z, Abrahamson NA (2011) Site-specific spectra for vertical ground motion. Earthq Spectra 27:1023–1047

Haji-Soltani A, Pezeshk S, Malekmohammadi M, Zandieh A (2017) A study of vertical-to-horizontal ratio of earthquake components in the Gulf Coast Region. Bull Seismol Soc Am 107(5):2055–2066. https://doi.org/10.1785/0120160252

Joyner WB, Boore DM (1981) Peak horizontal acceleration and velocity from strong-motion records including records from the 1979 Imperial Valley, California, earthquake. Bull Seism Soc Am 71:2011–2038

Kunnath SK, Erduran E, Chai YH, Yashinsky M (2008) Effect of near-fault vertical ground motions on seismic response of highway overcrossings. J Bridge Eng ASCE 13:282–290

Laouami N, Slimani A, Larbes S (2018) Ground motion prediction equations for Algeria and surrounding region using site classification based H/V spectral ratio. Bull Earthq Eng 16:2653–2684. https://doi.org/10.1007/s10518-018-0310-3

Newmark NM, Hall WJ (1982) Earthquake spectra and design. Earthquake Engineering Research Institute, Berkeley

Papazoglou AJ, Elnashai AS (1996) Analytical and field evidence of the damageng effect of vertical earthquake ground motion. Earthq Eng Struct Dyn 25:1109–1137

RPA99 (2003) Règlement Parasismique Algérien. CGS Earthquake Engineering Research Center, Rue Kaddour Rahim, BP 252, Hussein Dey, Algiers, Algeria

Sabetta F, Lucantoni A, Bungum H, Bommer J (2005) Sensitivity of PSHA results to ground motion prediction relations and logic-tree weights. Soil Dyn Earthq Eng 25:317–329. https://doi.org/10.1016/j.soildyn.2005.02.002

SESAME (2004) Guidelines for the implementation of H/V spectral ratio technique on ambient vibration measurements, processing and interpretation. Available at: http://sesame-fp5.obs.ujf-grenoble.fr/Deliverables/Del-D23-HV_User_Guidelines.pdf. Last Accessed July 2011

Spudich P, Fletcher JB, Hellweg M, Boatwright J, Sullivan C, Joyner WB, Hanks TC, Boore DM, McGarr A, Baker LM, Lindh AG (1997) SEA96-A new predictive relation for earthquake ground motion in extensional tectonic regimes. Seism Res Lett 68:190–198

Stewart JP, Boore DM, Seyhan E, Atkinson GM (2016) NGA-West2 equations for predicting vertical-component PGA, PGV, and 5%-Damped PSA from shallow crustal earthquakes. Earthq Spectra 32(2):1005–1031

Zhao JX, Irikura K, Zhang J, Fukushima Y, Somerville PG, Asano A et al (2006) An empirical site-classification method for strong strong-motion stations in Japan using H/V response spectral ratio. Bull Seismol Soc Am 96:914–925

Zhao JX, Jiang F, Ma Y, Zhou J, Cheng Y, Chang Z (2017) Ground-motion prediction equations for the vertical component from shallow crustal and upper-mantle earthquakes in Japan using site classes as the site term. Bull Seismol Soc Am 107(5):2310–2327. https://doi.org/10.1785/0120160376

Affiliations

Nasser Laouami[1]

[1] Centre National de Recherche Appliquée en Génie Parasismique (CGS), BP.232, 16040 Hussein Dey, Algiers, Algeria